



OPEN ACCESS

EDITED BY

Xin Ye, The First Affiliated Hospital of Xi'an Jiaotong University, China

REVIEWED BY

Dehashis Dutta University of Nebraska Medical Center, **United States** Siriruk Changrob,

Cornell University, United States

*CORRESPONDENCE

Peiming Zheng ™zpm8266@163.com Jing Zhao

⊠ zj971@126.com

Fenaxia Guo

guoxia0312@163.com

[†]These authors have contributed equally to this work

RECEIVED 03 April 2025 ACCEPTED 20 October 2025 PUBLISHED 04 November 2025

CITATION

Yuan Y, Geng Y, Rong T, Wang B, Mao X, Zhang X, Zhang X, Zhang Y, Zheng P, Zhao J and Guo F (2025) Novel method for the identification of circulating SARS-CoV-2 variants and clinical characteristics of patient infection with SARS-CoV-2 variants in Central China. Front, Cell, Infect, Microbiol, 15:1605198 doi: 10.3389/fcimb.2025.1605198

COPYRIGHT

© 2025 Yuan, Geng, Rong, Wang, Mao, Zhang, Zhang, Zhang, Zheng, Zhao and Guo. This is an open-access article distributed under the terms of the Creative Commons Attribution License (CC BY). The use, distribution or reproduction in other forums is permitted, provided the original author(s) and the copyright owner(s) are credited and that the original publication in this journal is cited, in accordance with accepted academic practice. No use. distribution or reproduction is permitted which does not comply with these terms.

Novel method for the identification of circulating SARS-CoV-2 variants and clinical characteristics of patient infection with SARS-CoV-2 variants in Central China

Youhua Yuan 1,2,3†, Yiman Geng 1,2,3†, Tingjun Rong 4†, Baoya Wang^{1,2,3}, Xiaohuan Mao^{1,2,3}, Xiaohuan Zhang^{1,2,3}, Xiulei Zhang^{1,2,3}, Yuan Zhang^{1,2,3}, Peiming Zheng^{1,2,3*}, Jing Zhao 1,2,3* and Fengxia Guo 1,2,3*

¹Department of Laboratory, Henan Provincial People's Hospital, Zhengzhou, Henan, China, ²Department of Laboratory, People's Hospital of Zhengzhou University, Zhengzhou, Henan, China, ³Department of Laboratory, People's Hospital of Henan University, Zhengzhou, Henan, China, ⁴Department of Laboratory, Xinyang Municipal Central Hospital, Xinyang, Henan, China

Introduction: We established a reliable and cost-effective method for identifying severe acute respiratory syndrome coronavirus 2 variants circulating in central China and analysed the clinical characteristics of patients with acute coronavirus disease 2019 who were infected with these variants.

Methods: The RNA of centrifuged and enriched samples was extracted and reverse transcribed into cDNA. cDNA was then analysed using a nested polymerase chain reaction amplification and Sanger sequencing method targeting specific mutations in the spike, ORF1a, and N genes. This was validated against next-generation sequencing, achieving 100% concordance.

Results: Among 172 isolates, JN.1.18.2 was the most prevalent (52.9%, 91/172), followed by XDV.1 (25.0%, 43/172), JN.1.16 (20.9%, 36/172), and KP.2 (1.2%, 2/172), which was found in central China for the first time. Fever with cough (52.6%, 80/ 152) was the most common symptom and 59.9% (91/152) of patients had underlying conditions. JN.1.18.2-infected patients more frequently presented with double-lung computed tomography changes. A strong positive correlation was observed between the duration from hospital admission to the detection of SARS-CoV-2 variants and total hospitalisation duration.

Discussion: The new method provides a reliable tool for variant detection, highlighting milder clinical presentations in patients with active infections. Long-term monitoring of variants and patient characteristics is essential for effective prevention and treatment strategies.

acute coronavirus disease 2019, SARS-CoV-2 variant, nested PCR, next generation sequencing, clinical characteristic

1 Introduction

Coronavirus disease 2019 (COVID-19) rapidly spread across countries, causing a global pandemic (Ali et al., 2024). Severe acute respiratory syndrome coronavirus 2(SARS-CoV-2), a positive-stranded RNA virus that causes COVID-19, undergoes continuous evolution owing to the lack of proofreading by its RNA replicase, leading to mutations during transmission. Key mutations can increase viral infectivity, accelerate transmission, and drastically alter epidemic dynamics (Altare et al., 2024). The World Health Organization designated certain strains as "variants of concern" in November 2024 owing to their increased transmissibility, shorter incubation periods, and higher disease severity, contributing to epidemic rebounds globally (Hageman and Alcocer Alkureishi, 2022; Meganck et al., 2024; Wei et al., 2024).

The Omicron variant (B.1.1.529), first reported in South Africa on November 24, 2021, was detected in 57 countries by December 8, 2024 (Dai et al., 2024). Omicron replicates 70 times faster in human bronchial tissue than Delta (B.1.617.2), providing a significant transmission advantage (Ma et al., 2022; ML et al., 2024). Strengthening surveillance of viral mutations, assessing biological characteristics of variants, and developing vaccines are critical priorities for global epidemic control (Chen et al., 2024; Duan et al., 2024; Planas et al., 2024a). In May 2021, China issued the COVID-19 Prevention and Control Plan (version 8), emphasising SARS-CoV-2 variant surveillance and vaccine efficacy assessment (Chen et al., 2020; Han and Wu, 2024).

Currently, metagenomic next-generation sequencing (mNGS) is the gold standard for identifying viral variants by sequencing the full viral genome (Donzelli et al., 2022). Although advances in sequencing technology have simplified operations, mNGS remains expensive owing to high equipment, chip, and reagent costs and lacks the rapid throughput needed for immediate variant detection (Tartanian et al., 2023). Alternative methods for variant identification have been proposed but often lack reproducibility (Carattini et al., 2023; Nasereddin et al., 2022; Shen et al., 2024; Specchiarello et al., 2023; Wacharapluesadee et al., 2023).

Henan Province, located in central China with a population of 99 million (2024), remains underexplored in terms of clinical data on SARS-CoV-2 variants. Henan Provincial People's Hospital, a tertiary care centre in Zhengzhou with 6,000 beds, serves critically ill patients across the 17 cities in this region. However, no studies have analysed the clinical characteristics of patients infected with SARS-CoV-2 variants in this region.

In this study, we established a novel nested polymerase chain reaction (PCR) and Sanger sequencing method to target partial gene sequences of the spike, N, and ORF1a regions, enabling the identification of circulating SARS-CoV-2 variants. Additionally, we examined the clinical characteristics of patients infected with different variants in central China, offering valuable insights for clinicians and public health policymakers to enhance control and treatment strategies.

2 Materials and methods

2.1 Sample collection

In total, 172 samples from 152 patients with confirmed COVID-19 and 5 negative SARS-CoV-2 throat swab isolates were collected between June 1, 2024 and January 31, 2025. These samples were obtained from the Department of PCR at Henan Provincial People's Hospital. Additionally, to evaluate the specificity of SARS-CoV-2 variant identification, 45 positive isolates of other common respiratory pathogens were included. These comprised 10 influenza A (Flu A) throat swabs, 5 influenza B (Flu B) throat swabs, 5 respiratory syncytial virus (RSV) throat swabs, 5 *Mycoplasma* throat swabs, and 5 *Mycobacterium tuberculosis* sputum samples, which were sourced from the microbiology laboratory between June 1, 2024 and January 31, 2025.

2.2 RNA extraction and reverse transcription

Throat swab samples (2.6 mL of virus reserve liquid) or sputum samples (1 mL) were centrifuged at 15,000 × g for 1.5 h or not centrifuged, respectively. A 300- μ L aliquot was subjected to RNA extraction using a nucleic acid extraction kit (Zhijiang Ltd., Shanghai, China) with an automatic extraction system (EX3600, Shanghai ZJ Bio-Tech Co., Ltd., Shanghai, China). The final RNA pellet was dissolved in 50 μ L of RNase-free water and 10 μ L of extracted RNA was reverse-transcribed into cDNA using a reverse transcriptase PCR kit (Mighty Script Plus Mix, Sangon Biotech Co., Ltd., Shanghai, China) and thermal cycler (T100, Bio-Rad, Hercules, CA, USA).

2.3 Primer design and validation

As most mutation points among SARS-CoV-2 variants are located in the spike, N, and ORF1a regions(https://gisaid.org/ lineage-comparison/), in this study, genomic differences in the spike, N, and ORF1a regions among SARS-CoV-2 variants circulating in central China (June 2024 to January 2025) were analysed using online databases and https://ngdc.cncb.ac.cn/ncov/ monitoring/country/China). Thirteen specific mutation points were selected (seven in the spike protein, four in the N protein, and one in the ORF1a protein) (Figure 1). Oligo 7 (version 7.60, Molecular Biology Insights, Toronto, Canada) was used to design seven nested PCR primer sets targeting these mutations based on the SARS-CoV-2 reference genome (MN908947, GenBank, Bethesda, MD, USA). Specificity was confirmed using NCBI Primer-BLAST (https:// www.ncbi.nlm.nih.gov/tools/primer-blast/). Primer details are provided in Table 1. The specificity of primers was validated through nested PCR (Figure 2) and Sanger sequencing (Figure 3).

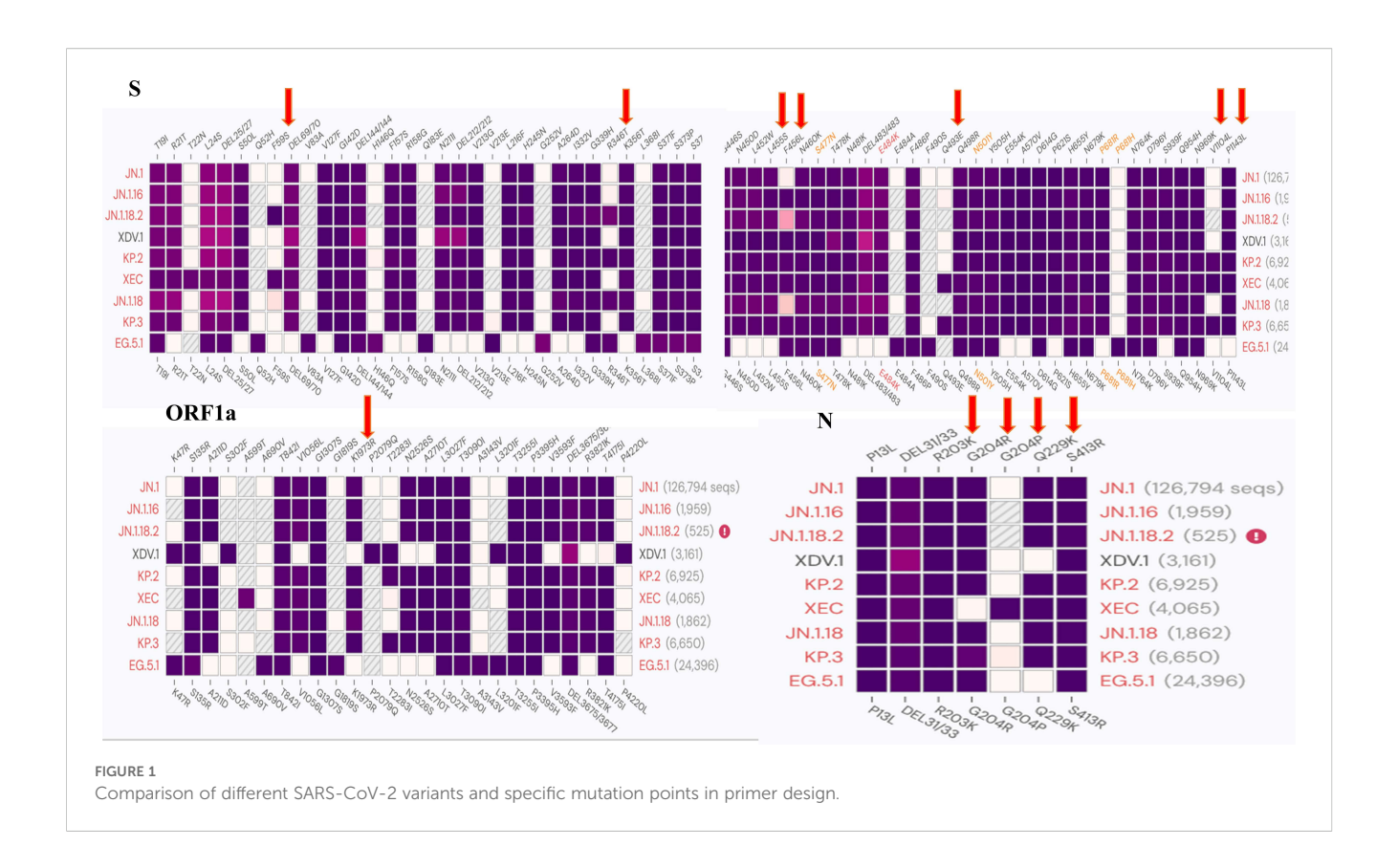


TABLE 1 Details of nested primers for identifying variants of SARS-CoV-2.

| Primer name | Amplifying area and position | Direction | Sequence (5'-3') | Annealing temperature | Product length | Specific point of variants |
|----------------|------------------------------|------------------------------|-------------------------|--------------------------|-------------------|----------------------------|
| O379 | ORF1a5768-6166 | F | CAAGCTTCGATAATTTTAAGTTT | 50 | 379 | K1973R |
| | | R | TAGGATTTTCCACTACTTCT | | | |
| O330n | ORF1a5793 -6142 | F | ATGTGATAATATCAAATTTGCT | 50 | 330 | |
| | | R | GACTGGTTTTAGATCTTCG | | | |
| O268 | ORF1a5752-6019 | F | CAACCATATCCAAACGCAAG | 50 | 268 | K1973R |
| | | R | TATTTGGTTTATACGTGGCT | | | |
| O190n | ORF1a5794-5983 | F | TGTGATAATATCAAATTTGCTG | 50 | 190 | |
| | | R | TAACATGCCAAACAATAGGT | | | |
| O220 | ORF1a5787-5807 | F | GTTTGTATGTGATAATATCAAA | 48 | 220 | K1973R |
| | | R | TGTTAACATGCCAAACAAT | | | |
| O156n | ORF1a5811-5967 | F | TGCTGATGATTTAAACCAGT | 50 | 156 | |
| | | R | GGTTTATGTAACAATTTAGCTC | | | |
| S334 | S83-416 | 83-416 F TACACTAATTCTTTCACAC | | 48 | 334 | F59S |
| | | R | AAAATGGATCATTACAAA | | | |
| S292n | \$105-396 | F | TGTTTATTACCCTGACAAA | 50 | 292 | _ |
| | | R | TTGAAATTCACAGACTTT | 1 | | |
| S229 | S81-309 | F | TACACTAATTCTTTCACACG | 48 | 229 | F59S |
| | | R | TGTTAGACTTCTCAGTGGAA | | | |

(Continued)

TABLE 1 Continued

| Primer name | Amplifying area and position | Direction | Sequence (5'-3') | Annealing temperature | Product length | Specific point of variants | |
|----------------|------------------------------|-------------------------|------------------------|-----------------------|-------------------|----------------------------|--|
| S161n | S103-263 | F | GTGTTTATTACCCTGACAAA | 50 | 161 | | |
| | | R | CATCATTAAATGGTAGGACA | | | | |
| S202 | S81-283 | F | ATACACTAATTCTTTCACACG | 48 | 202 | F59S | |
| | | R | GGAAGCAAAATAAACACCATC | | | | |
| S135n | S103-238 | F | GGTGTTTATTACCCTGACA | 50 | 135 | | |
| | | R | AAACCTCTTAGTACCATTGGTC | | | | |
| S220 | S1331-1551 | F | GCATAGTGGTAATTATGAT | 48 | 220 | Q493E | |
| | | R | TAGAAGTTCAAAAGAAAGTAC | | | | |
| S178n | S1352-1530 | F | ACTGGTATAGATCGCTTAGG | 50 | 178 | | |
| | | R | ACTACTCTGTATGGTTGGT | | | | |
| S300 | S1262-1561 | F | ATAATTATAAATTACCAGATGA | 48 | 300 | L455S | |
| | | R | GTGCATGTAGAAGTTCAAA | = | | F456L Q493E | |
| S248n | S1287-1534 | F | TACAGGCTGCGTTATAGCTT | 48 | 248 | | |
| | | R | CTACTACTCTGTATGGTTGG | | | | |
| S210 | S1235-1444 | F | CAGGGCAAACTGGAAA | 50 | 210 | L455S F456L | |
| | | R | CTTTACAAGGTTTGTTACCG | _ | | | |
| S159n | S1265-1423 | F | ATTATAAATTACCAGATGATT | 50 | 159 | | |
| | | R | CCTGATAGATTTCAGTTGA | | | | |
| S280 | S1276-1556 | F | CCAGATGATTTTACAGG | 48 | 280 | L455S, F456L, Q493E | |
| | | R | GTAGAAGTTCAAAAGAAAG | | | | |
| S242n | S1294-1536 | F | TGCGTTATAGCTTGGAA | 50 | 242 | | |
| | | R | ACTACTACTCTGTATGGT | = | | | |
| S301 | S3218-3517 | F | AGAACTTCACAACTGC | 48 | 301 | P1143L, V1104L | |
| | | R | TAATGCCAGAGATGTCA | | | | |
| S265-1n | S3235-3499 | F | CCTGCCATTTGTCATG | 48 | 265 | | |
| | | R | CTAAATCAACATCTGGT | | | | |
| S265 | S3242-3506 | F | TTTGTCATGATGGAAAAGCAC | 48 | 265 | P1143L | |
| | | R | ATGTCACCTAAATCAACATCTG | - | | | |
| S200n | S3264-3463 | F | CTTTCCTCGTGAAGGTGTC | 48 | 200 | | |
| | | R | ATTTATCTAACTCCTCCTTGAA | | | | |
| S260 | S928-1188 | F AAGGAATCTATCAAACTTC 4 | 48 | 260 | R346T | | |
| | | R | ATAGACATTAGTAAAGCAGA | - | | | |
| S216n | S949-1164 | F | AACTTTAGAGTCCAACCAA | 48 | 216 | | |
| | | R | ATTTAATTTAGTAGGAGACAC | | | | |
| S250 | S933-1182 | F | AATCTATCAAACTTCTAACTT | 50 | 250 | R346T | |
| 3230 | | R | ATTAGTAAAGCAGAGATCATT | | | | |
| S195n | S956-1150 | F | GAGTCCAACCAACAGAATC | 50 | 195 | - | |
| 31/311 | | R | GAGACACTCCATAACACTT | _ | | | |

(Continued)

TABLE 1 Continued

| Primer name | Amplifying area and position | Direction | Sequence (5′-3′) | Annealing temperature | Product length | Specific point of variants |
|----------------|------------------------------|-----------|------------------------|--------------------------|-------------------|----------------------------|
| N343 | N536-878 | F | GCAGTCAAGCCTCTTCTCGTT | 50 | 343 | G204R G204P |
| | | R | CTGATTAGTTCCTGGTCCCCAA | | | Q229K |
| N280n | N561-840 | F | CTCATCACGTAGTCGCAACAG | 50 | 280 | |
| | | R | TGGACCACGTCTGCCGAAA | | | |

2.4 Nested PCR amplification of Spike, N, and ORF1a regions

A standard nested PCR protocol was developed to amplify the spike, N, and ORF1a regions of SARS-CoV-2. In the first round, 4 μ L of template cDNA was amplified using 2× SanTaq PCR mixture (Sangon Biotech Co, Shanghai, China) in a thermal cycler (T100, Bio-Rad, Hercules, CA, USA). The thermal cycling parameters were as follows: pre-denaturation at 94°C for 5 min, 60 cycles of denaturation at 94°C for 30 s, annealing at 48°C for 30 s, and extension at 72°C for 18 s, followed by a final extension at 72°C for 10 min. For the second round, 10 μ L of the first-round product was used as the template, with the same thermal cycling conditions except for a different denaturation temperature (50°C).

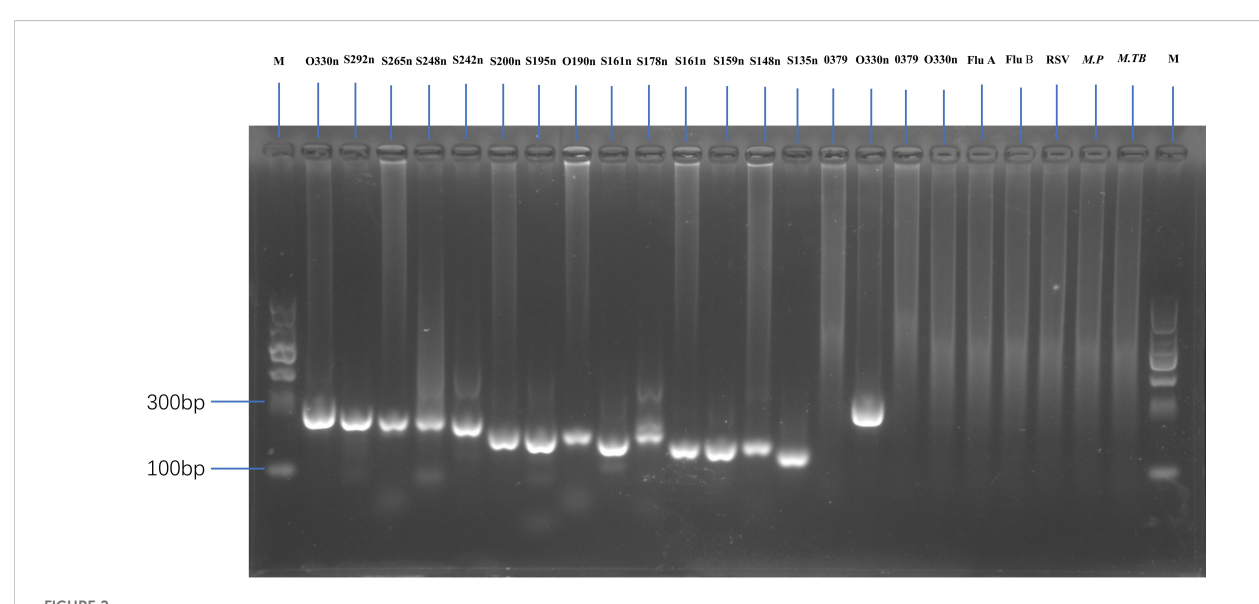
The nested PCR products were analysed via 1.5% agarose gel electrophoresis at $110~\rm V$ for 35 min (Figure 2).

2.5 Sanger sequencing of SARS-CoV-2 Spike, N, and ORF1a protein partial genomes

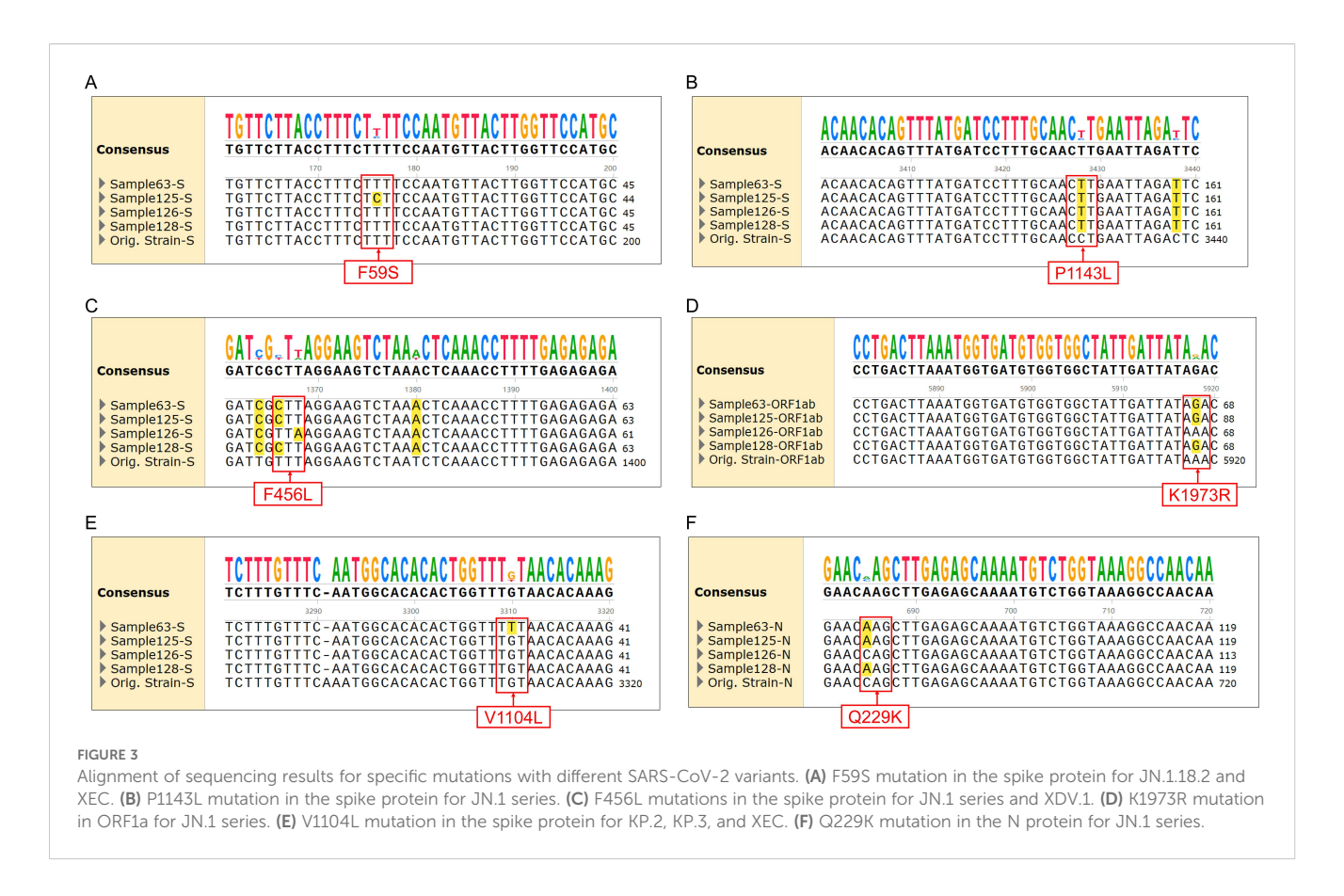
Positive nested PCR products were subjected to Sanger sequencing at Shanghai Sangon Biotech (Shanghai, China) to analyse the partial genomes of the targeted spike, N, and ORF1a regions using the corresponding forward primer sets listed in Table 1.

2.6 Validation of the Sanger sequencing strategy for SARS-CoV-2 variant screening

To validate the accuracy of SARS-CoV-2 variant identification through nested amplification, 16 positive samples were analysed via NGS performed by Shanghai Sangon Biotech (Shanghai, China)



Gel electrophoresis showing amplification fragments of varying lengths by nested PCR. M, 1 to 24 panels represent DNA markers with fragment lengths of O330n, S292n, S265n, S248n, S242n, S200n, S195n, O190n, S161n, S178n, S161n, S159n, S148n, S135n, and O379 (first-round PCR product with centrifugation), O330 (second-round PCR product with centrifugation), O379 (first-round PCR product without centrifugation), and O330 (second-round PCR product without centrifugation) bp. Other lanes represent a negative SARS-CoV-2 sample, as well as Flu A, Flu B, RSV, Mycoplasma pneumoniae (M.P), and Mycobacterium tuberculosis (M. TB) samples.



and Zhengzhou Auto Diag Biotech (Zhengzhou, China) (Table 2). Whole-genome sequences were uploaded to the PANGOLIN platform (https://pangolin.cog-uk.io/) for variant identification.

2.7 Classification of notable SARS-CoV-2 variants

Classification criteria for notable SARS-CoV-2 variants are outlined in Table 3. Samples were first amplified using seven nested primer sets to generate longer fragments. For samples that failed to produce the expected longer fragments, alternative nested primer sets were used to generate shorter fragments. Twelve specific mutation points within these fragments were sequenced via Sanger sequencing and sequence alignment was conducted using SnapGene (version 6.02, GSL Biotech, Chicago, IL, USA). Mutations were compared against the reference SARS-CoV-2 genome (MN908947) from GenBank (https://www.ncbi.nlm.nih.gov/nuccore/MN908947) (Figure 3). By analysing combinations of these 13 mutation points (Table 4), notable SARS-CoV-2 variants, including those spreading in China (e.g., XDV.1, JN.18.2, KP.2), were identified. The schematic workflow is shown in Figure 4.

2.8 Clinical characteristics of hospitalised patients with COVID-19 who were infected with SARS-CoV-2 variants

Clinical data for 132 hospitalised patients and 20 patients hospitalised in a fever clinic with confirmed SARS-CoV-2 infection

were retrieved from the electronic medical record system of our hospital (Hospital Information System). Variables collected included age, sex, city of residence in Henan Province, duration from admission to positive SARS-CoV-2 sample, underlying comorbidities, symptoms, treatment outcomes, cycle threshold (Ct) values for the *ORF1a* and *N* genes, hospitalisation duration, and computed tomography (CT) features. Additionally, one set of laboratory data, including white blood cell (WBC), lymphocyte, and platelet counts and C-reactive protein (CRP), procalcitonin, alanine aminotransferase, D-dimer, IL-6, and lactate dehydrogenase concentrations, was collected on the test date with the shortest interval from the date of a SARS-CoV-2-positive test result. These data were analysed to characterise clinical differences among patients infected with distinct SARS-CoV-2 variants.

2.9 Definition of treatment outcomes and severity

Owing to traditional Chinese death culture, family members do not want the patient to die in the hospital and hope that the patient dies at home. Therefore, as the family members usually take the patient home prior to death, especially in rural areas, the cause of death is not clear in the medical records. Accordingly, we had to define treatment outcomes based on the medical records prior to death: voluntary discharge and discontinuation of treatment were defined as treatment failure, whereas treatment response leading to discharge was defined as treatment success. Additionally, we classified the patients into mild and severe cases according to the latest Chinese protocols for COVID-19 diagnosis

10.3389/fcimb.2025.1605198

Yuan et al.

| a, and N protein. |
|-------------------|
| ORF18 |
| ike protein, |
| he Spi |
| s of t |
| n point |
| mutation |
| specific |
| ts by |
| variant |
| -2 |
| CoV |
| SARS- |
| a of |
| criteri |
| Identification |
| TABLE 2 |

and treatment (Released by National Health Commission of People's Republic of China & National Administration of Traditional Chinese Medicine on January 5, 2023, 2023).

2.10 Statistical analysis

Summary statistics are presented as median with interquartile range or mean with standard error, depending on data distribution. Statistical significance among groups was assessed using the Kruskal–Wallis test with Bonferroni adjustments for continuous variables. Categorical variables were analysed using Pearson's χ^2 test or Fisher's exact test based on the feature of data. Correlations between continuous variables were evaluated using Spearman's rank correlation, with significance set at p<0.05. All statistical analyses were conducted using SPSS (version 25.0; IBM Corp., Armonk, NY, USA) and GraphPad Prism (version 8.0; La Jolla, CA, USA).

2.11 Ethical considerations

The study was approved by the Ethics Committee of Henan Provincial People's Hospital (Approval No. 241225). Written informed consent was obtained from all participants at the beginning of the study. All procedures adhered to the guidelines of the Declaration of Helsinki.

3 Results

3.1 Basic characteristics of patients infected with different SARS-CoV-2 variants

In total, 172 throat swab samples were collected from 152 patients with confirmed acute COVID-19 cases between June 1, 2024 and January 31, 2025. Among the 152 patients, 83 were men and 69 were women (median age, 67 years). Of these, 132 patients were hospitalised across 20 different inpatient wards, whereas 20 were treated in the fever clinic.

Twenty-six patients (17.1%, 26/152) had infections that were classified as severe cases requiring ICU admission and five patients died. In contrast, 82.9% (126/152) of the cases were classified as mild, based on the latest Chinese guidelines for the diagnosis and treatment of COVID-19 (Released by National Health Commission of People's Republic of China & National Administration of Traditional Chinese Medicine on January 5, 2023, 2023; Wu et al., 2023). No significant difference was observed in the incidence of severe disease among patients infected with the JN.1.18.2, XDV.1 and JN.1.16 variants (p = 0.249, Table 3).

The 152 cases were distributed across 17 cities in Henan Province, spanning all directions. Most patients (58.6%, 89/152) were from Zhengzhou, the provincial capital located centrally, followed by 17 (11.2%, 17/152) from the southern region of Henan Province. No significant differences in the distribution of SARS-CoV-2 variants were observed across regions in central China.

TABLE 3 Clinical characteristics of patients infected with different SARS-CoV-2 variants (N = 152 patients).

| Characteristics | JN.1.18.2 (n=76) | XDV.1 (n=39) | JN.1.16 (n=35) | KP.2 (n=2) | Total (N = 152) | P-value |
|---|---------------------|-----------------|-------------------|---------------|--------------------|---------|
| Sex | | | | | | |
| Men | 45 | 20 | 18 | 0 | 83 | 0.383 |
| Women | 31 | 19 | 17 | 2 | 69 | |
| Age | 67 (57.3–77.5) | 65 (51–74) | 60 (41-73) | 39 (20–39) | 66.5 (51.5–75) | 0.091 |
| Family location in Henan Province | | | | | | |
| East | 12 | 4 | 8 | 0 | 24 | 0.130 |
| West | 3 | 3 | 3 | 1 | 10 | |
| South | 14 | 2 | 1 | 0 | 17 | |
| North | 7 | 2 | 3 | 0 | 12 | |
| Centre | 40 | 28 | 20 | 1 | 89 | |
| Signs and symptoms | | | | | | |
| Fever | 16 | 14 | 14 | 0 | 44 | 0.144 |
| Cough | 1 | 0 | 0 | 0 | 1 | |
| Fever and cough | 48 | 17 | 14 | 1 | 80 | |
| None | 11 | 8 | 7 | 1 | 27 | |
| Lung CT change | | | | | _ | |
| Single | 7 | 3 | 1 | 0 | 11 | 0.045 |
| Double | 49 | 20 | 15 | 0 | 84 | |
| None | 20 | 16 | 19 | 2 | 57 | |
| Hospitalised days | 12 (7–24) | 11 (7–20) | 9 (6–13) | 16 (9–16) | 10 (6–18) | 0.279 |
| Days from admission to positive SARS-CoV-2 sample | 5 (1–10) | 4 (1-8) | 2 (1-7) | 7.5 (3–7.5) | 4 (1-9) | 0.368 |
| Underlying diseases | | | | | | |
| Hypertension | 36 | 15 | 10 | 1 | 62 | 0.252 |
| Diabetes | 25 | 6 | 6 | 0 | 37 | 0.110 |
| Cerebral fraction | 15 | 9 | 4 | 0 | 28 | 0.594 |
| Coronary heart disease | 17 | 6 | 10 | 0 | 28 | 0.516 |
| Number of underlying diseases | | ' | | | <u>'</u> | ' |
| 0 | 23 | 20 | 17 | 1 | 61 | 0.443 |
| 1 | 25 | 7 | 6 | 1 | 39 | |
| 2 | 11 | 6 | 5 | 0 | 22 | |
| 3 | 13 | 5 | 7 | 0 | 25 | |
| 4 | 4 | 1 | 0 | 0 | 5 | |
| Hospitalised ward | | | | | | |
| Internal | 49 | 30 | 19 | 2 | 100 | 0.318 |
| Surgery | 2 | 1 | 3 | 0 | 6 | |
| ICU | 17 | 3 | 6 | 0 | 26 | |
| Fever clinic | 8 | 5 | 7 | 0 | 20 | |

(Continued)

TABLE 3 Continued

| Characteristics | JN.1.18.2 (n=76) | XDV.1 (n=39) | JN.1.16 (n=35) | KP.2 (n=2) | Total (N = 152) | P-value | | | |
|----------------------------|---------------------|------------------|-------------------|------------------|--------------------|---------|--|--|--|
| Classification of severity | | | | | | | | | |
| Mild | 63 | 31 | 30 | 2 | 126 | 0.850 | | | |
| Severe | 13 | 8 | 5 | 0 | 26 | | | | |
| Outcomes | Outcomes | | | | | | | | |
| Treatment success | 65 | 34 | 32 | 2 | 133 | 0.821 | | | |
| Treatment failure | 11 | 5 | 3 | 0 | 19 | | | | |
| Ct value | | | | | | | | | |
| ORF1a gene | 19.7 (16.1-23.3) | 20.5 (15.5–23.6) | 15.4 (13.7-23.0) | 15.2 (10.3–15.2) | 18.1 (14.3-21.9) | 0.295 | | | |
| N gene | 19.1 (15.5–22.9) | 20.5 (14.3-23.5) | 15.7 (13.1–21.4) | 14.3 (9.4–14.3) | 19.9 (14.8-23.0) | 0.308 | | | |

The most common symptom was fever with cough (52.6%, 80/152). Additionally, 59.9% (91/152) of the patients had at least one underlying disease. Lung CT showed single or bilateral abnormalities in 62.5% (95/152) of the patients, whereas 37.5% (57/152) had no CT abnormalities. The median hospitalisation duration was 11 (interquartile range [IQR]: 7–20) days and the median interval from admission to a positive SARS-CoV-2 test was 4 (IQR: 1–9) days. Detailed clinical characteristics of patients infected with different SARS-CoV-2 variants are provided in Table 3.

3.2 Sensitivity and specificity of nested PCR for identifying SARS-CoV-2 variants

Nested PCR was performed for all 217 samples using the same primer set and reaction parameters. Among the 172 confirmed SARS-CoV-2-positive samples, all (100%, 172/172) were successfully amplified and sequenced using this method, indicating a sensitivity rate of 100%. Conversely, no amplification products were detected for the 45 pathogen-positive but SARS-CoV-2-negative samples, confirming a specificity rate of 100% (45/45).

Additionally, we compared the PCR results of samples with and without centrifugation. The amplification of expected fragments in first- and second-round PCR was more successful with centrifuged samples than with non-centrifuged samples (Figure 2, lane 15-18).

3.3 Concordance rate of SARS-CoV-2 variants identified by nested reverse transcription (RT)-PCR and NGS

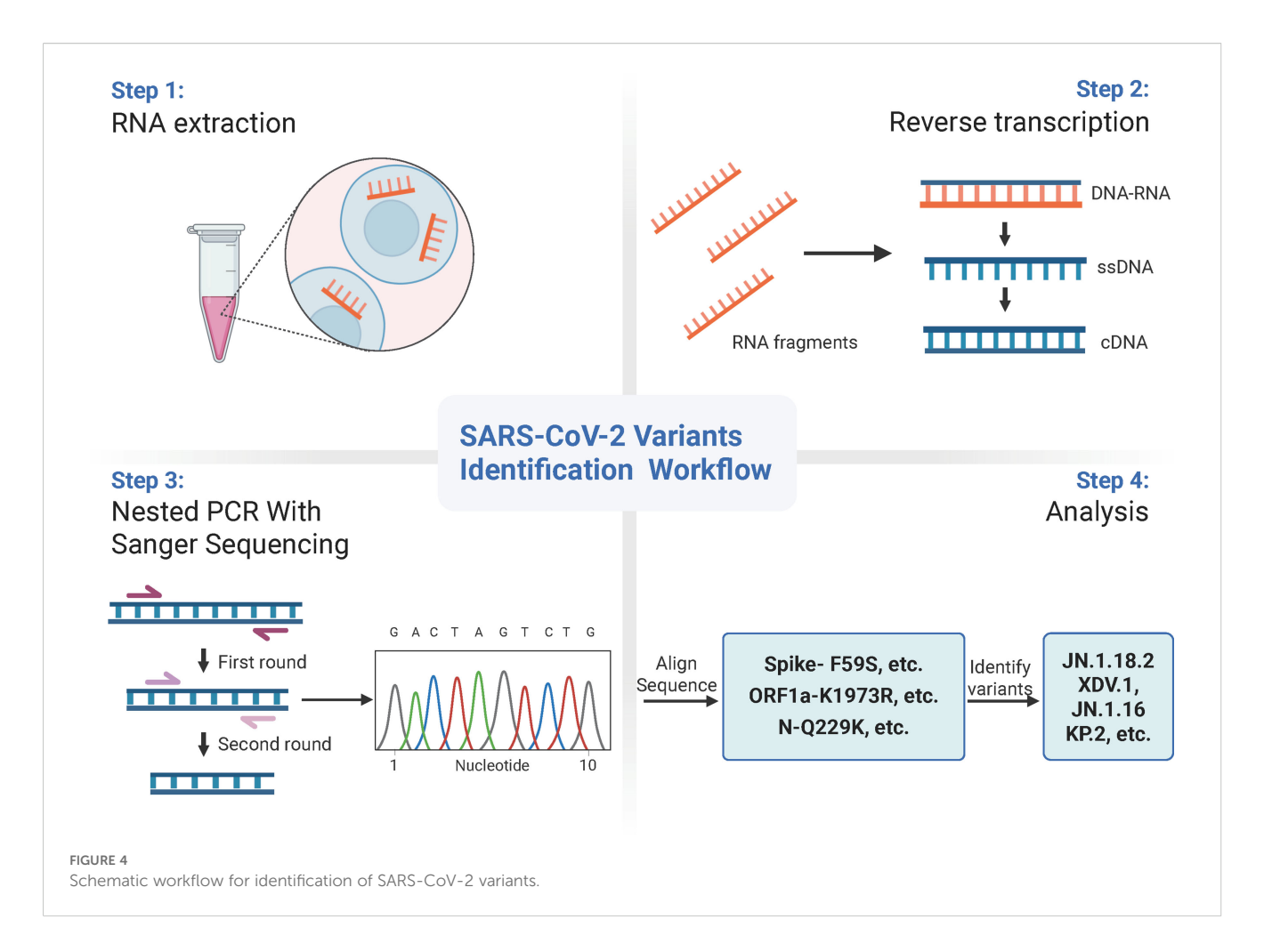
We compared the results between NGS and nested PCR followed by Sanger sequencing, which showed 100% (16/16) concordance between the methods (Figure 5).

3.4 Distribution of notable SARS-CoV-2 variants

Among the 172 isolates screened, the most prevalent variant was JN.1.18.2, characterised by a specific F59S mutation in the spike protein (Figure 3A), accounting for 52.9% (91/172) of the isolates.

TABLE 4 Clinical characteristics of patients infected with different SARS-CoV-2 variants (N = 152 patients) (continued).

| Characteristics | JN.1.18.2 (n=76) | XDV.1 (n=39) | JN.1.16 (n=35) | KP.2 (n=2) | Total (N = 152) | P-value |
|---|---------------------|-------------------|-------------------|------------------|--------------------|---------|
| Laboratory detection results | | | | | | |
| WBC count (109/L) Median (p25, p75) | 8.8 (6.7, 8.9) | 6.8 (4.8, 9.3) | 6.4 (3.5, 7.7) | 5.2 (4.3, 7.4) | 6.7 (4.9, 8.9) | 0.148 |
| Lymphocyte count (10 ⁹ /L) Median (p25, p75) | 0.9 (0.8, 1.6) | 0.8 (0.3, 1.1) | 1.3 (0.4, 1.5) | 1.2 (0.7, 2.2) | 0.9 (0.6, 1.4) | 0.426 |
| Platelet count (10 ⁹ /L) Median (p25, p75) | 256 (187, 320) | 95 (60.8, 162) | 208 (144, 248) | 221 (181, 251) | 180 (124, 238) | 0.060 |
| CRP (ng/mL) Median (p25, p75) | 18.4 (13.8, 176) | 39.8 (13.8, 71.7) | 12.2 (3.5, 25.3) | 17.2 (3.4, 31.9) | 15.0 (4.1, 43.9) | 0.676 |
| Procalcitonin (ng/mL) Median (p25, p75) | 0.7 (0.1, 1.4) | 0.5 (0.2, 1.5) | 0.1 (0.05, 0.1) | 0.05 (0.02, 0.1) | 0.11 (0.05, 0.5) | 0.127 |
| D-dimer (ng/mL) Median (p25, p75) | 2.2 (0.9, 6.9) | 2.1 (0.8, 4.6) | 2.8 (0.2, 8.5) | 0.7 (0.2, 1.2) | 1.6 (0.6, 3.96) | 0.080 |
| IL-6 (ng/mL) Median (p25, p75) | 22.5 (13.18, 73.0) | 60.2 (9.8, 280) | 42.7 (1.4, 181) | _ | 22.5 (5.8, 182) | 0.215 |
| Alanine transaminase (IU/mL) Median (p25, p75) | 17.0 (12.8, 27.6) | 13.0 (10.6, 52.9) | 20.6 (12.4, 31.0) | 9.9 (8.8, 38.8) | 21.7 (12.4, 50) | 0.189 |
| Lactate dehydrogenase (IU/mL) Median (p25, p75) | 226 (210, 355) | 244 (203, 319) | 217 (160, 278) | 166 (160, 237) | 221 (182, 259) | 0.376 |



This was followed by the XDV.1 variant (25.0%, 43/172) and JN.1.16 variant (20.9%, 36/172), which harboured specific L455S and F456L spike protein mutations. Additionally, a K1973R mutation in the ORF1a region was observed in the JN.1.16, JN.1.18.2, and KP.2 variants (Figures 3B–D). Two isolates were identified as variants of KP.2, which was found in Henan Province in central China for the first time, characterised by V1104L spike protein and Q229K N protein mutations (Figures 3E, F, Figure 6A).

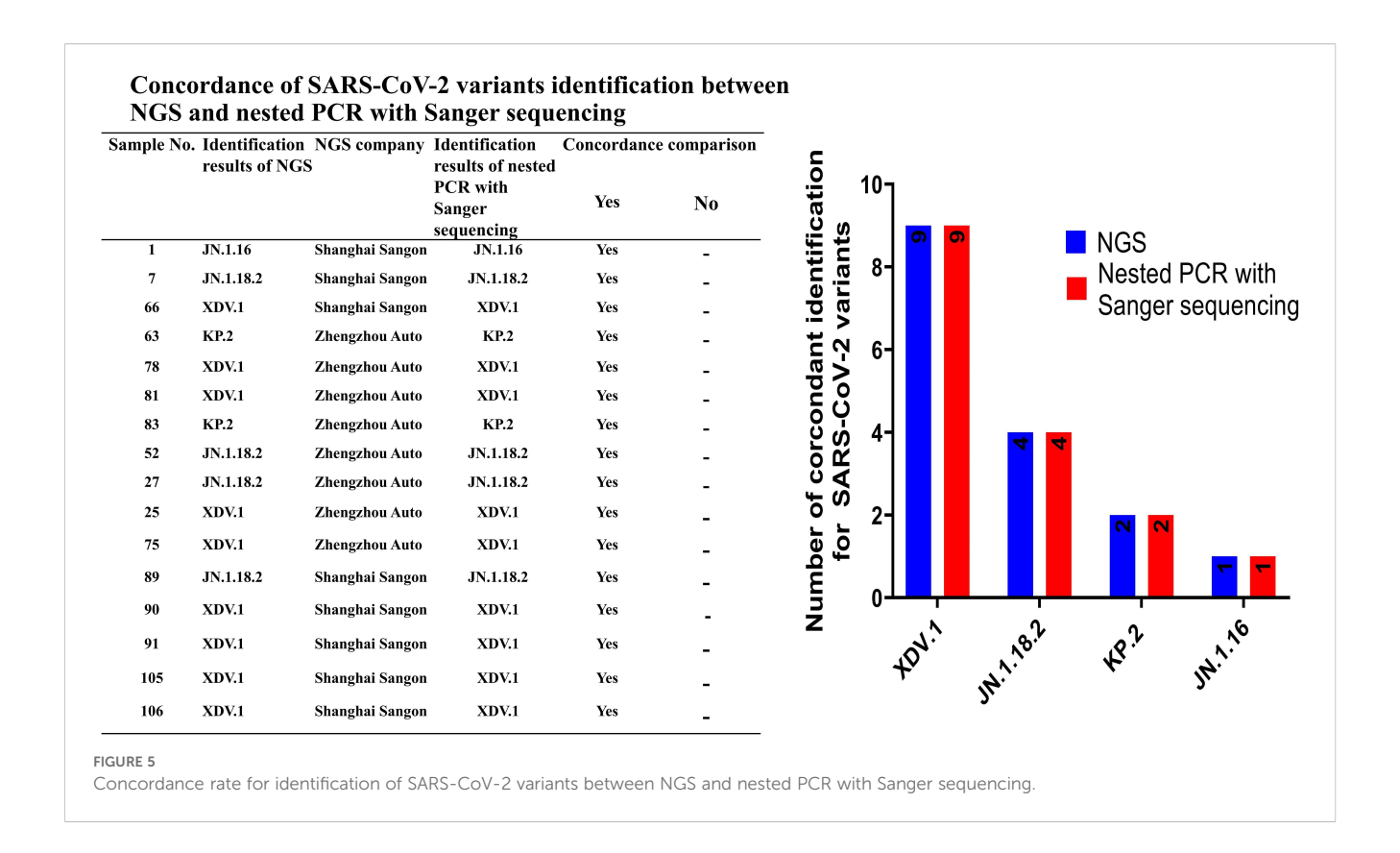
The prevalence of SARS-CoV-2 and proportion of different variants varied significantly across months from June 2024 to January 2025. The highest positivity rate for SARS-CoV-2 infection occurred in August 2024, reaching 24.9% (59/237) (p=0.034, Figure 6B, Supplementary Table S1). In January 2025, the JN.1.18.2 variant accounted for 95.8% (23/24) of cases, representing its highest monthly proportion (Figure 6C).

3.5 Clinical characteristics of patients infected with SARS-CoV-2 variants

In total, 64.5% (49/76) of patients infected with the JN.1.18.2 variant exhibited bilateral lung abnormalities on CT, which was significantly higher than the 46.1% (35/76) observed in patients

infected with other variants (p=0.045, Figure 6D). Moreover, there was a strong positive correlation between the duration from hospital admission to the detection of SARS-CoV-2 variants and total hospitalisation duration ($r=0.81,\ p<0.001$, Figure 6E). Similarly, a strong positive linear correlation was observed between the Ct values of the ORF1a and N genes in patients infected with different SARS-CoV-2 variants (Figure 6F, $r=0.997,\ p<0.001$). Additionally, a significant positive linear relationship was found for the Ct values of ORF1a between patients infected with the XDV.1 and JN.1.16 variants (Supplementary Figure S1A, $r=0.64,\ p<0.001$).

No significant differences were observed in the age or geographic location distribution among patients infected with different SARS-CoV-2 variants (p=0.091 and p=0.383, respectively, Figures 7A–D). Additionally, no significant differences were found in underlying comorbidities (hypertension, diabetes, coronary heart disease, or cerebral infarction) and clinical symptoms (fever or cough) among patients infected with different variants (Figures 7E, F). Similarly, no significant differences were observed in Ct values of the ORF1a and N genes (Supplementary Figures S1B–F, p=0.110 and p=0.594, respectively), disease severity classification, treatment outcome, ward distribution, number of comorbidities, hospitalisation duration, or time from



admission to the detection of positive samples among patients infected with different SARS-CoV-2 variants (p = 0.279 to p = 0.850, respectively, Supplementary Figures S2A-F).

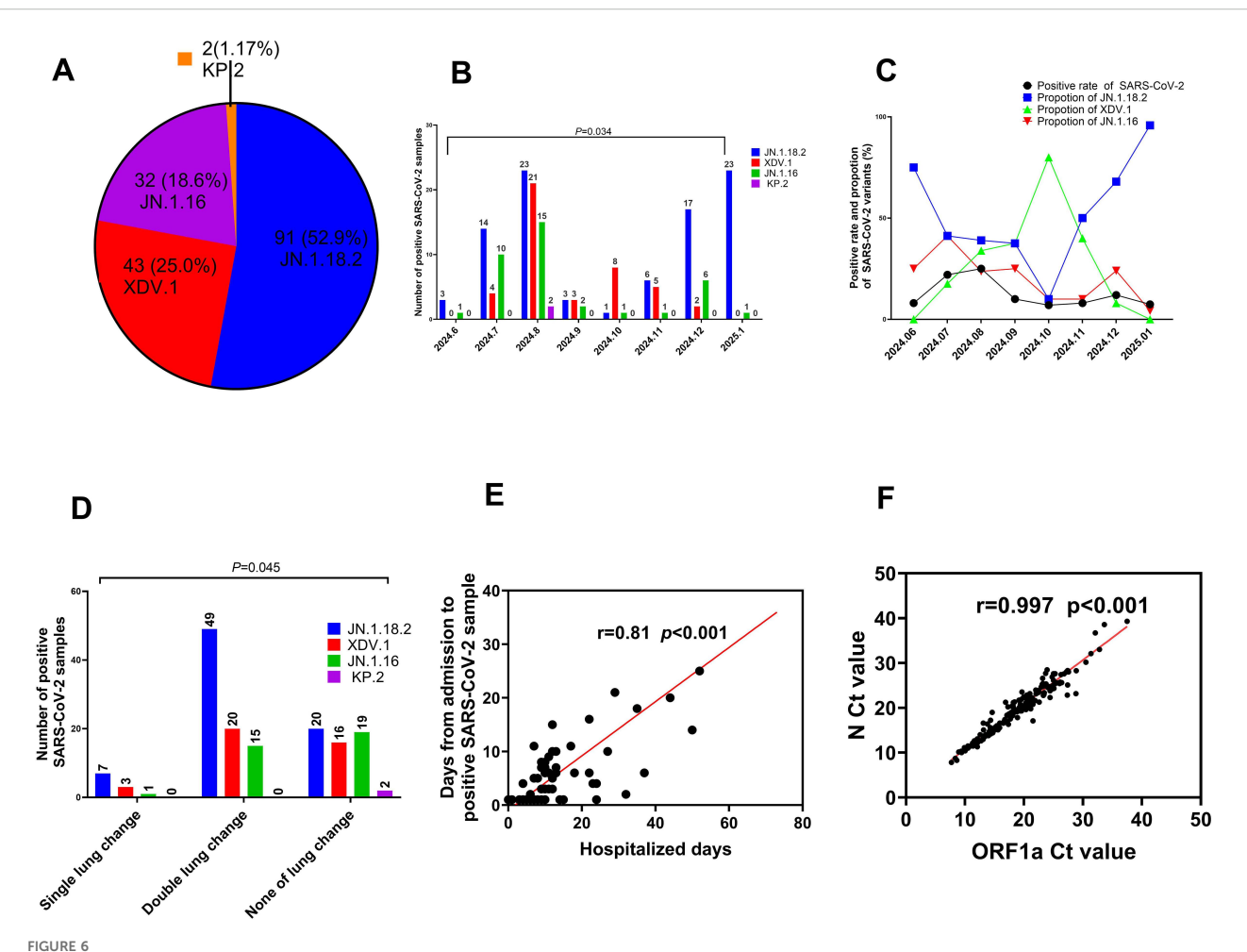
Laboratory detection results, including alanine aminotransferase concentration; WBC, lymphocyte, and platelet counts; and CRP, procalcitonin, D-dimer, IL-6, and lactate dehydrogenase concentrations, did not significantly differ among patients infected with different SARS-CoV-2 variants (p = 0.418 to p = 0.410, Table 4, Supplementary Figures S3A–I).

4 Discussion

In this study, we reported a novel nested PCR method for identifying SARS-CoV-2 variants circulating in central China and described the primary clinical characteristics of patients with acute COVID-19 who were infected with different variants. Our established method provides a reliable tool to monitor the evolutionary trends of SARS-CoV-2 within the population and serves as a reference for the development of vaccines targeting specific variants. Additionally, our findings on the clinical characteristics of different variants contribute valuable data for epidemic control measures and optimising the allocation of medical resources for patients with COVID-19. To the best of our knowledge, this is the first report to establish a nested PCR method for identifying circulating SARS-CoV-2 variants and describe the clinical characteristics of patients with acute COVID-19 who were infected with these variants in China.

Although several methods, including ordinary PCR sequencing, real-time quantitative PCR, and digital PCR, have been reported for identifying SARS-CoV-2 variants (Berno et al., 2022; Chhoung et al., 2024; Martínez-Murcia et al., 2023; Wu et al., 2023), our preliminary experiments revealed that many of the primers and protocols described in the literature were unable to amplify the expected PCR fragments. The primary limitation of previously reported methods was that their amplified fragments were often too long, reaching lengths of up to 600 base pairs (bp) (Martínez-Murcia et al., 2022). Another issue was that the primers used in these methods were often designed to amplify the variants prevalent in specific regions at the time of the studies. Over time, the composition of circulating variants has evolved and many primers now overlap with mutation points, rendering them ineffective for identifying current variants (Chhoung et al., 2024; Martínez-Murcia et al., 2022, 2023). To address these limitations, we self-designed our primers and established a robust nested PCR method capable of reliably identifying circulating SARS-CoV-2 variants in central China.

From our practical experience, the main challenges in clinical SARS-CoV-2-positive specimens include low viral loads and the poor integrity of extracted RNA templates. To overcome these issues, we enriched the virus content in the specimen by centrifugation at $15,000 \times g$ for 1.5 h, increased the sensitivity of amplification, and developed a two-round nested PCR method with validated superiority in sensitivity and specificity. The key advantage of our method lies in its shorter amplification fragments: the maximum length was 330 bp (targeting the ORF1a



Comparison of key clinical characteristics among different SARS-CoV-2 variants. (A) Total proportion of different SARS-CoV-2 variants from June 2024 to January 2025. (B) Distribution of SARS-CoV-2 variants by month from June 2024 to January 2025. (C) Comparison of positive SARS-CoV-2 sample rates and constituent proportions of different variants from June 2024 to January 2025. (D) Comparison of age distribution among patients with COVID-19 who were infected with different SARS-CoV-2 variants. (E) Relationship between the Ct values of ORF1a and N gene. (F) Comparison of Ct values among patients with COVID-19 who were infected with different SARS-CoV-2 variants.

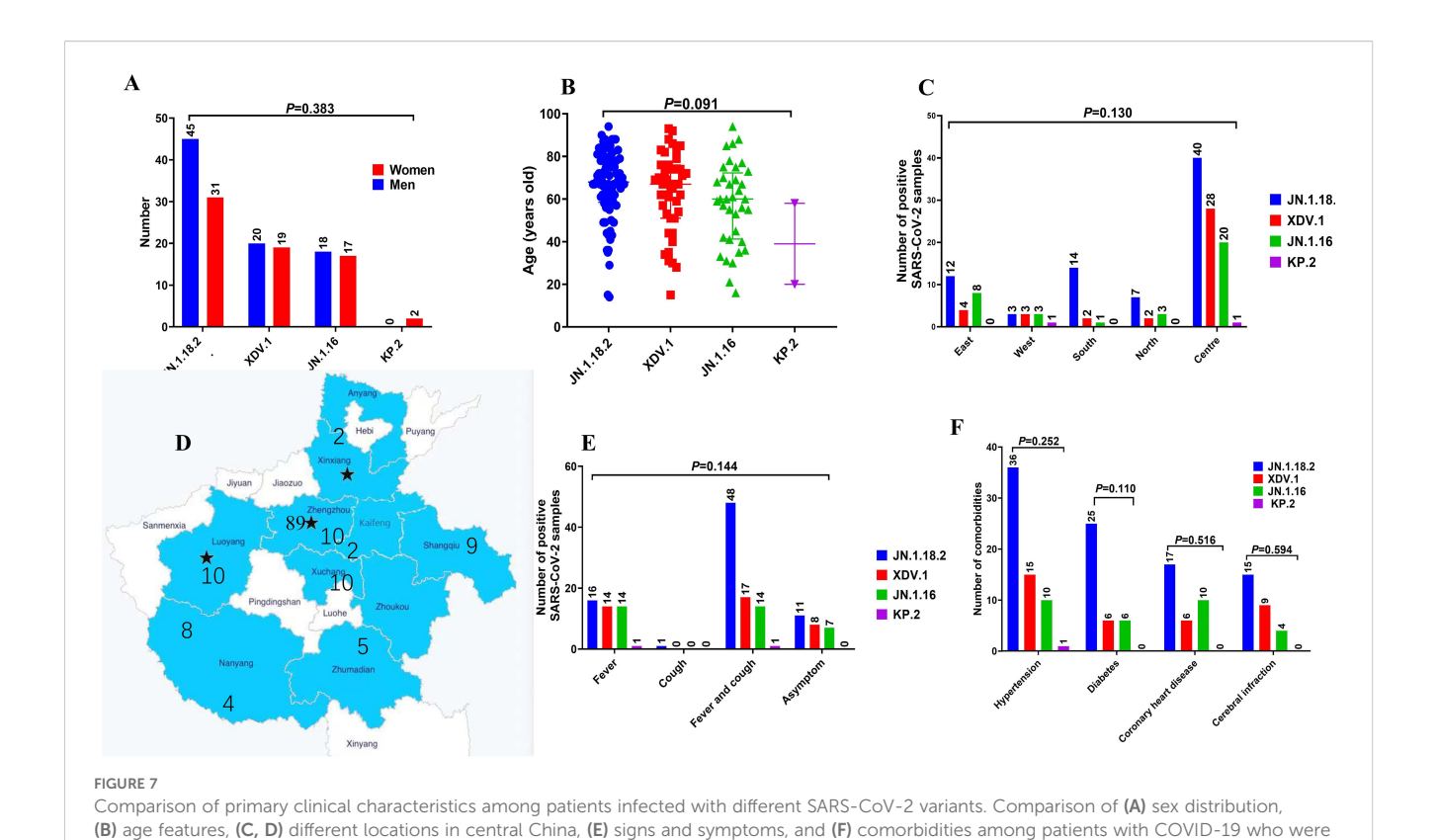
site) and minimum length was 135 bp (targeting the spike protein site). We observed that shorter amplified fragments significantly increased the probability of successful amplification. To improve success rates, we designed alternative primer sets for each specific site, achieving a 100% identification success rate. This is also our first attempt to create a method of increasing virus concentration by centrifugation (Martínez-Murcia et al., 2022, 2023).

Unlike a previous study that focused solely on amplifying the spike protein to identify SARS-CoV-2 variants (Martínez-Murcia et al., 2022), our method incorporates additional mutation points in the ORF1a and N domains alongside those in the spike protein. This addition was crucial because we found that some variants, such as JN.1.16 and XDV.1, share identical spike protein mutations. Amplifying only the spike protein would have led to a failure in differentiating these two variants. This significant observation, which has not been reported in previous studies, underscores the importance of including multiple target regions for accurate variant identification.

Our results demonstrated that the proportion of the JN.1.18.2 variant in central China was higher than that of XDV.1, which

contrasts with the most recent surveillance data released by the Chinese Center for Disease Control and Prevention (2025). According to the SARS-CoV-2 variant monitoring data from December 2024 by the Chinese CDC, the XDV.1 series accounted for a higher proportion (59.1%) across the entire country than the JN.1 series (37.6%), which includes the JN.1.18.2, JN.1.16, and KP.2 variants. This regional difference may be attributed to the specific geographic characteristics of Henan Province, which is centrally located in China. We identified two isolates of the KP.2 variant, which was previously prevalent in India and the United States (Kaku et al., 2024; Karyakarte et al., 2024; Kumar et al., 2024) but had only been found in limited quantities in coastal areas such as Guangdong, China. To the best of our knowledge, this is the first report of the KP.2 variant in Henan Province.

Regarding the clinical characteristics of 152 patients with COVID-19, our data showed that fever with cough was the most common symptom across infections with various SARS-CoV-2 variants. No significant difference was observed in signs and symptoms, mortality among severe cases, underlying conditions,



treatment outcomes, nine laboratory detection results, or length of hospitalisation among patients infected with different variants. However, for older individuals with multiple underlying conditions, COVID-19 caused by various SARS-CoV-2 variants can still result in severe disease or even death (Planas et al., 2024b). Among the 26 patients with severe disease in our cohort, four died after infection with the JN.1.18.2 variant and one with the XDV.1 variant. Overall, as SARS-CoV-2 has evolved, the severity of COVID-19 has generally decreased, whereas the transmission potential of variants appears to be increasing. This trend is consistent with findings from other regions worldwide (Hughes et al., 2023; Kuthning et al., 2024).

infected with different SARS-CoV-2 variants.

Our findings revealed that patients infected with the JN.1.18.2 variant exhibited more double-lung CT changes than those infected with the XDV.1 and JN.1.16 variants. This observation has not yet been reported. We hypothesise that the JN.1.18.2 variant, with mutations such as F59S and L455S in the spike protein, may have a stronger immune escape capacity than the XDV.1 and JN.1.16 variants. This could explain why JN.1.18.2 is more likely to infect individuals with compromised immunity, such as older people and those with diabetes (Carey et al., 2022; Hasanzad et al., 2022; Liu et al., 2024). Additionally, we observed a strong correlation between the duration from admission to the detection of positive specimens and length of hospitalisation, suggesting that some patients acquired their infections in hospital settings. Given the recent shift in COVID-19 control measures from dynamic zero-COVID to routine epidemic control, infection rates among patients have increased compared with those in 2022 (Xu et al., 2024). This poses particular risks for older patients with underlying conditions. Routine epidemic controls highlight the need for strengthened infection control measures, particularly for hospitalised older patients, and education on self-protection measures, such as mask-wearing and maintaining social distancing. Furthermore, the development of a broad-spectrum COVID-19 vaccine is essential to address the continuous emergence of new SARS-CoV-2 variants (Chang et al., 2024; Link-Gelles et al., 2024; Subissi et al., 2024; Wu et al., 2022).

There are some limitations to our study. First, our research primarily focused on the identification of notable SARS-CoV-2 variants in China, which may have led to the exclusion of rare mutations or variants found in other regions, such as Africa and America (Aggarwal et al., 2023; Mboowa et al., 2024; Santoni, 2024; Zhao et al., 2022). Future studies will explore additional primers and real-time probe PCR methods to identify emerging SARS-CoV-2 variants globally. Second, our sample size and collection duration were relatively small. We plan to continue sample collection over a longer period to validate the reliability of our established method. Lastly, we will monitor genomic sequence trends, mutation patterns, and clinical manifestations of emerging variants to inform clinical strategies and policy decisions for COVID-19 control and treatment.

In conclusion, this study demonstrates the reliability and practicality of nested PCR with Sanger sequencing for screening samples for notable SARS-CoV-2 variants. Compared with NGS and other methods, our approach offers a cost-effective, universally applicable, and time-efficient tool for identifying emerging variants, particularly in regions where NGS may not be accessible. Through this method, we identified JN.1.18.2 and XDV.1 as the most prevalent SARS-CoV-2 variants in central China, with a smaller

proportion of KP.2 variants. Moreover, patients infected with the JN.1.18.2 variant were more likely to have bilateral lung abnormalities on CT than those infected with the XDV.1 and JN.1.16 variants; therefore, early variant detection will enable clinicians to treat patients better, thereby avoiding severe COVID-19 and death. Although acute COVID-19 cases caused by these variants presented with milder symptoms than those caused by earlier strains, older patients with underlying conditions such as diabetes should be closely monitored for early diagnosis and treatment to prevent progression to severe disease.

Data availability statement

The original contributions presented in the study are included in the article/Supplementary Material. Further inquiries can be directed to the corresponding authors.

Ethics statement

The studies involving humans were approved by Henan Provincial People's Hospital. The studies were conducted in accordance with the local legislation and institutional requirements. The participants provided their written informed consent to participate in this study.

Author contributions

YY: Conceptualization, Data curation, Formal Analysis, Investigation, Methodology, Project administration, Software, Writing - original draft, Writing - review & editing. YG: Conceptualization, Data curation, Investigation, Project administration, Resources, Supervision, Writing - original draft, Writing - review & editing. TR: Data curation, Methodology, Writing - review & editing. BW: Funding acquisition, Methodology, Visualization, Writing - review & editing. XM: Formal Analysis, Investigation, Methodology, Validation, Writing - review & editing. XHZ: Funding acquisition, Investigation, Supervision, Writing review & editing. XLZ: Data curation, Methodology, Project administration, Software, Validation, Writing - review & editing. YZ: Funding acquisition, Resources, Supervision, Visualization, Writing - review & editing. PZ: Funding acquisition, Investigation, Resources, Writing - review & editing. JZ: Project administration, Resources, Supervision, Writing - review & editing. FG: Funding acquisition, Investigation, Writing - review & editing.

Funding

The author(s) declare financial support was received for the research and/or publication of this article. This work was supported

by the National Natural Science Foundation of China (82002199), Key Project of Medical Science and Technology of Henan Province (LHGJ20230009), Henan Province Youth and Middle-aged Health Science and Technology Innovation Program (YQRC2023017), and Science and Technology Tackling in Henan Province (232102310084). The funders had no role in study design, data collection and interpretation, or the decision to submit the work for publication.

Acknowledgments

We thank all study participants, volunteers, partners, the Henan Provincial People's Hospital Data Safety Monitoring Board, and the study steering committee. In addition, we are grateful to our partners, Wenjing Wang, Sheng Zhan from Auto Diag company, and Shanshan Liu from our laboratory department, who assisted with instruments and some reagents of the experiments.

Conflict of interest

The authors declare that the research was conducted in the absence of any commercial or financial relationships that could be construed as a potential conflict of interest.

Generative Al statement

The author(s) declare that no Generative AI was used in the creation of this manuscript.

Any alternative text (alt text) provided alongside figures in this article has been generated by Frontiers with the support of artificial intelligence and reasonable efforts have been made to ensure accuracy, including review by the authors wherever possible. If you identify any issues, please contact us.

Publisher's note

All claims expressed in this article are solely those of the authors and do not necessarily represent those of their affiliated organizations, or those of the publisher, the editors and the reviewers. Any product that may be evaluated in this article, or claim that may be made by its manufacturer, is not guaranteed or endorsed by the publisher.

Supplementary material

The Supplementary Material for this article can be found online at: https://www.frontiersin.org/articles/10.3389/fcimb.2025.1605198/full#supplementary-material

References

(2023). Released by National Health Commission of People's Republic of China & National Administration of Traditional Chinese Medicine on January 5, 2023. *Health Care Sci.* 2, 10–24. doi: 10.1002/hcs2.36

Aggarwal, N. R., Molina, K. C., Beaty, L. E., Bennett, T. D., Carlson, N. E., Mayer, D. A., et al. (2023). Real-world use of nirmatrelvir-ritonavir in outpatients with COVID-19 during the era of omicron variants including BA.4 and BA.5 in Colorado, USA: A retrospective cohort study. *Lancet Infect. Dis.* 23, 696–705. doi: 10.1016/S1473-3099 (23)00011-7

Ali, S. T., Chen, D., Lau, Y. C., Lim, W. W., Yeung, A., Adam, D. C., et al. (2024). Insights into COVID-19 epidemiology and control from temporal changes in serial interval distributions in Hong Kong. *Am. J. Epidemiol.* 194, 1079–1089. doi: 10.1093/aje/kwae220

Altare, C., Kostandova, N., Basadia, L. M., Petry, M., Gankpe, G. F., Crockett, H., et al. (2024). COVID-19 epidemiology, health services utilisation and health care seeking behaviour during the first year of the COVID-19 pandemic in Mweso health zone, Democratic Republic of Congo. *J. Glob. Health* 14, 5016. doi: 10.7189/jogh.14.05016

Berno, G., Fabeni, L., Matusali, G., Gruber, C. E. M., Rueca, M., Giombini, E., et al. (2022). SARS-CoV-2 variants identification: Overview of molecular existing methods. *Pathogens* 11, 1058. doi: 10.3390/pathogens11091058

Carattini, Y. L., Griswold, A., Williams, S., Valiathan, R., Zhou, Y., Shukla, B., et al. (2023). Combined use of RT-qPCR and NGS for identification and surveillance of SARS-CoV-2 variants of concern in residual clinical laboratory samples in Miami-Dade County, Florida. *Viruses* 15, 593. doi: 10.3390/v15030593

Carey, L. B., Koenig, H. G., Gabbay, E., Hill, T., Cohen, J., Aiken, C., et al. (2022). Nursing, diabetes, hemodialysis and COVID-19. *J. Relig. Health* 61, 1767–1771. doi: 10.1007/s10943-022-01586-6

Chang, T. Y., Li, C. J., Chao, T. L., Chang, S. Y., and Chang, S. C. (2024). Design of the conserved epitope peptide of SARS-CoV-2 spike protein as the broad-spectrum COVID-19 vaccine. *Appl. Microbiol. Biotechnol.* 108, 486. doi: 10.1007/s00253-024-13331-y

Chen, Z., Du, L. Z., Fu, J. F., Shu, Q., Chen, Z. M., Shi, L. P., et al. (2020). Emergency plan for inter-hospital transfer of newborns with SARS-CoV-2 infection. *Zhong Guo Dang Dai Er Ke Za Zhi* 22, 226–230. doi: 10.7499/j.issn.1008-8830.2020.03.009

Chen, L., He, Y., Liu, H., Shang, Y., and Guo, G. (2024). Potential immune evasion of the severe acute respiratory syndrome coronavirus 2 Omicron variants. *Front. Immunol.* 15. doi: 10.3389/fimmu.2024.1339660

Chhoung, C., Ko, K., Ouoba, S., Phyo, Z., Akuffo, G. A., Sugiyama, A., et al. (2024). Sustained applicability of SARS-CoV-2 variants identification by Sanger sequencing strategy on emerging various SARS-CoV-2 Omicron variants in Hiroshima, Japan. *BMC Genomics* 25, 1063. doi: 10.1186/s12864-024-10973-0

Chinese Center for Disease Control and Prevention (2025). *National novel coronavirus epidemic situation*. Available online at: https://www.Chinacdc.cn/jksj/xgbdyq/202501/t20250107_303736.html (Accessed February 30, 2025).

Dai, B., Ji, W., Zhu, P., Han, S., Chen, Y., and Jin, Y. (2024). Update on Omicron variant and its threat to vulnerable populations. *Public Health Pract.* 7, 100494. doi: 10.1016/j.puhip.2024.100494

Donzelli, S., Ciuffreda, L., Pontone, M., Betti, M., Massacci, A., Mottini, C., et al. (2022). Optimizing the Illumina COVIDSeq laboratorial and bioinformatics pipeline on thousands of samples for SARS-CoV-2 variants of concern tracking. *Comp. Struct. Biotechnol. J.* 20, 2558–2563. doi: 10.1016/j.csbj.2022.05.033

Duan, H., Zhang, E., Ren, G., Cheng, Y., Yang, B., Liu, L., et al. (2024). Exploring immune evasion of SARS-CoV-2 variants using a pseudotyped system. *Heliyon* 10, e29939. doi: 10.1016/j.heliyon.2024.e29939

Hageman, J. R., and Alcocer Alkureishi, L. (2022). Omicron: A variant of concern? *Pediatr. Ann.* 51, el. doi: 10.3928/19382359-20211207-03

Han, L., and Wu, F. (2024). COVID-19 drives medical education reform to promote 'healthy China 2030' action plan. *Front. Public Health* 12. doi: 10.3389/fpubh.2024.1465781

Hasanzad, M., Larijani, B., and Aghaei Meybodi, H. R. (2022). Diabetes and COVID-19: A bitter nightmare. *J. Diabetes Metab. Disord.* 21, 1191–1193. doi: 10.1007/s40200-022-00994-5

Hughes, T. D., Subramanian, A., Chakraborty, R., Cotton, S. A., Herrera, M. D. P. G., Huang, Y., et al. (2023). The effect of SARS-CoV-2 variant on respiratory features and mortality. *Sci. Rep.* 13, 4503. doi: 10.1038/s41598-023-31761-y

Kaku, Y., Uriu, K., Kosugi, Y., Okumura, K., Yamasoba, D., Uwamino, Y., et al. (2024). Virological characteristics of the SARS-CoV-2 KP.2 variant. *Lancet Infect. Dis.* 24, e416. doi: 10.1016/S1473-3099(24)00298-6

Karyakarte, R. P., Das, R., Potdar, V., Kulkarni, B., Joy, M., Mishra, M., et al. (2024). Tracking KP.2 SARS-coV-2 variant in India and the clinical profile of KP.2 cases in maharashtra, India. *Cureus* 16, e66057. doi: 10.7759/cureus.66057

Kumar, P., Jayan, J., Sharma, R. K., Gaidhane, A. M., Zahiruddin, Q. S., Rustagi, S., et al. (2024). The emerging challenge of FLiRT variants: KP.1.1 and KP.2 in the global pandemic landscape. *Q.J.M.* 117, 485–487. doi: 10.1093/qjmed/hcae102

Kuthning, D., Raafat, D., Holtfreter, S., Gramenz, J., Wittmann, N., Bröker, B. M., et al. (2024). Variant-specific antibody profiling for tracking SARS-CoV-2 variant infections in children and adolescents. *Front. Immunol.* 15. doi: 10.3389/fimmu.2024.1434291

Link-Gelles, R., Ciesla, A. A., Mak, J., Miller, J. D., Silk, B. J., Lambrou, A. S., et al. (2024). Early Estimates of Updated 2023–2024 (Monovalent XBB.1.5) COVID-19 vaccine effectiveness against symptomatic SARS-CoV-2 infection attributable to cocirculating omicron variants among immunocompetent adults – Increasing community access to testing program, United States, September 2023-January 2024. MMWR Morb. Mortal. Wkly. Rep. 73, 77–83. doi: 10.15585/mmwr.mm7304a2

Liu, Y., Zhao, X., Shi, J., Wang, Y., Liu, H., Hu, Y. F., et al. (2024). Lineage-specific pathogenicity, immune evasion, and virological features of SARS-CoV-2 BA.2.86/JN.1 and EG.5.1/HK.3. *Nat. Commun.* 15, 8728. doi: 10.1038/s41467-024-53033-7

Ma, W., Yang, J., Fu, H., Su, C., Yu, C., Wang, Q., et al. (2022). Genomic perspectives on the emerging SARS-CoV-2 omicron variant. *Genomics Proteomics Bioinf.* 20, 60–69. doi: 10.1016/j.gpb.2022.01.001

Martínez-Murcia, A., Garcia-Sirera, A., Navarro, A., and Pérez, L. (2022). SARS-CoV-2 variants identification; A fast and affordable strategy based on partial S-gene targeted PCR sequencing. *Viruses* 14, 2588. doi: 10.3390/v14112588

Martínez-Murcia, A., Garcia-Sirera, A., Navarro, A., and Pérez, L. (2023). Correction: Martínez-Murcia, A., Garcia-Sirera, A., Navarro, A., and Pérez, L. SARS-CoV-2 variants identification; A fast and affordable strategy based on partial S-gene targeted PCR sequencing. *Viruses* 14, 2588. doi: 10.3390/v14112588

Mboowa, G., Kakooza, F., Egesa, M., Tukwasibwe, S., Kanyerezi, S., Sserwadda, I., et al. (2024). The rise of pathogen genomics in Africa. F1000Research 13, 468. doi: 10.12688/f1000research.147114.2

Meganck, R. M., Edwards, C. E., Mallory, M. L., Lee, R. E., Dang, H., Bailey, A. B., et al. (2024). SARS-CoV-2 variant of concern fitness and adaptation in primary human airway epithelia. *Cell Rep.* 43, 114076. doi: 10.1016/j.celrep.2024.114076

M L, S. P., Kumari, S., Martinek, T. A., and M, E. S. (2024). De novo design of potential peptide analogs against the main protease of Omicron variant using in silico studies. *Phys. Chem. Chem. Phys.* 26, 14006–14017. doi: 10.1039/d4cp01199f

Nasereddin, A., Golan Berman, H., Wolf, D. G., Oiknine-Djian, E., and Adar, S. (2022). Identification of SARS-CoV-2 variants of concern using amplicon next-generation sequencing. *Microbiol. Spec.* 10, e0073622. doi: 10.1128/spectrum.00736-22

Planas, D., Staropoli, I., Michel, V., Lemoine, F., Donati, F., Prot, M., et al. (2024b). Distinct Evol. SARS-CoV-2 Omicron XBB and BA.2.86/JN.1 lineages combining increased fitness and antibody evasion. *Nat. Commun.* 15, 2254. doi: 10.1038/s41467-024-46490-7

Planas, D., Staropoli, I., Planchais, C., Yab, E., Jeyarajah, B., Rahou, Y., et al. (2024a). Escape of SARS-coV-2 variants KP.1.1, LB.1, and KP3.3 from approved monoclonal antibodies. *Pathog. Immun.* 10, 1–11. doi: 10.20411/pai.v10i1.752

Santoni, D. (2024). An entropy-based study on the mutational landscape of SARS-CoV-2 in USA: Comparing different variants and revealing co-mutational behavior of proteins. *Gene* 922, 148556. doi: 10.1016/j.gene.2024.148556

Shen, S., Fu, A. Y., Jamba, M., Li, J., Cui, Z., Pastor, L., et al. (2024). Rapid detection of SARS-CoV-2 variants by molecular-clamping technology-based RT-qPCR. *Microbiol. Spec.* 12, e0424823. doi: 10.1128/spectrum.04248-23

Specchiarello, E., Matusali, G., Carletti, F., Gruber, C. E. M., Fabeni, L., Minosse, C., et al. (2023). Detection of SARS-CoV-2 variants *via* different diagnostics assays based on single-nucleotide polymorphism analysis. *Diagnostics* 13, 1573. doi: 10.3390/diagnostics13091573

Subissi, L., Otieno, J. R., Worp, N., Attar Cohen, H., Oude Munnink, B. B., Abu-Raddad, L. J., et al. (2024). An updated framework for SARS-CoV-2 variants reflects the unpredictability of viral evolution. *Nat. Med.* 30, 2400–2403. doi: 10.1038/s41591-024-02040.

Tartanian, A. C., Mulroney, N., Poselenzny, K., Akroush, M., Unger, T., Helseth C.OMMAJr., D. L., et al. (2023). NGS implementation for monitoring SARS-CoV-2 variants in Chicagoland: An institutional perspective, successes and challenges. *Front. Public Health* 11. doi: 10.3389/fpubh.2023.1177695

Wacharapluesadee, S., Hirunpatrawong, P., Petcharat, S., Torvorapanit, P., Jitsatja, A., Thippamom, N., et al. (2023). Simultaneous detection of omicron and other SARS-CoV-2 variants by multiplex PCR MassARRAY technology. *Sci. Rep.* 13, 2089. doi: 10.1038/s41598-023-28715-9

Wei, H., Zhao, Y., Rui, J., Li, K., Abudunaibi, B., Zhao, Z., et al. (2024). Transmissibility of the variant of concern for SARS-CoV-2 in six regions. *Heliyon* 10, e32164. doi: 10.1016/j.heliyon.2024.e32164

Wu, Y., Feng, X., Gong, M., Han, J., Jiao, Y., Li, S., et al. (2023). Evolution and major changes of the diagnosis and treatment protocol for COVID-19 patients in China 2020–2023. *Health Care Sci.* 2, 135–152. doi: 10.1002/hcs2.45

Wu, Y., Wang, S., Zhang, Y., Yuan, L., Zheng, Q., Wei, M., et al. (2022). Lineage-mosaic and mutation-patched spike proteins for broad-spectrum COVID-19 vaccine. *Cell Host Microbe* 30, 1732–1744.e7. doi: 10.1016/j.chom.2022.10.011

Xu, J., Yuan, Y., Chen, G., Ma, B., Zou, Y. L., Wang, B., et al. (2024). Characteristics of humoral responses to the first coronavirus disease booster vaccine and breakthrough infection in central China: A multicentre, prospective, longitudinal cohort study. *Front. Immunol.* 15. doi: 10.3389/fimmu.2024.1446751

Zhao, L. P., Lybrand, T. P., Gilbert, P., Madeleine, M., Payne, T. H., Cohen, S., et al. (2022). Application of statistical learning to identify omicron mutations in SARS-CoV-2 viral genome sequence data from populations in Africa and the United States. *JAMA Netw. Open* 5, e2230293. doi: 10.1001/jamanetworkopen.2022.30293